Voltage Stability in a Photovoltaic-based DC Microgrid with GaN-Based Bidirectional Converter using Fuzzy Controller for EV Charging Applications

KOTTALA PADMA, KALANGIRI MANOHAR
Department of Electrical Engineering,
Andhra University College of Engineering, Andhra University, Visakhapatnam,
AndharPradesh,
INDIA

Abstract: - Electric vehicles are growing in importance owing to their desirable characteristics leading to utilization. It is a significant challenge to maintain voltage for DC microgrids when integrating with EVs. The work aims to enhance voltage stability in a DC microgrid and the electric vehicle charging using GaN devices in the converter. This is done by developing a DC microgrid with better voltage regulation, loss reduction, and increased efficiency and these are analyzed using PLECS software. Under different operating conditions, the proposed converter can respond to load fluctuations and maintain its voltage profile stable. The approach meets the increasing demand for vehicle charging by upgrading DC microgrid technology. The use of GaN-based converters improves voltage stability while allowing for efficient integration of EVs into the grid thereby giving more options for transportation.

Key-Words: - PI Controller, Fuzzy Controller, Gallium Nitride Bi-directional DC-DC Converters, Electrical Vehicles, PV Array, DC Microgrid, Voltage Stability.

Received: April 23, 2023. Revised: February 21, 2024. Accepted: March 27, 2024. Published: May 9, 2024.

1 Introduction

Evaluation of the reliability and safety of DC microgrid system, [1], [2], [3], depends on its DC bus voltage. However, in this process sudden changes in the power supply may lead to huge deviations from the normal levels of voltage for instance in service behavior and demand fluctuations. This emphasizes the need to maintain power quality as well as ensure that DC bus voltages remain stable. Therefore, a bidirectional (DC-DC) converter is employed to interface energy storage devices with the DC bus to tackle these issues, [4]. During the insertion of Energy Storage Devices (EDS) into a DC microgrid, the reliability is increased since it determines both the transmission power from the microgrid source and energy absorption power at load based on EDS size, [5]. Here, Solar DC Microgrid Solution ensures secure Voltage stability as well as good Power Quality. Reliable power supply as well as economic power management are rendered feasible through the integration of ESD to the microgrid via BDCs.

A closed loop controlling technique that concentrates on the parameters voltage along with current is utilized in recent converter designing. This approach often utilizes an updated version of this technique. In the realm of control theory, a method called closed-loop control is employed to handle both voltage and current. In this arrangement, the bus voltage takes on the role of the layer of control while a PI controller is used to compensate for any discrepancies, in the internal loop, [6]. Though this conventional control approach enhances the responsiveness of the system it still struggles to eradicate the notable fluctuations and impacts, on the voltage of the DC microgrid. Consequently, there is a need, for control mechanisms that can meet these requirements while also enhancing the stability and reliability of energy storage unit converters. Exploring more intricate and advanced methods, such as adaptive and predictive control approaches, could be investigated as potential solutions to address these challenges and enhance the performance of energy storage unit converters across various operating conditions.

Several researchers have used a system that blends classic dual closed-loop control techniques with the feedforward controlling technique to overcome this difficulty, [7]. Regardless of the feedforward components employed, these systems can be classified as power feedforward or current feedforward. For example, three feedforward load

current control strategies were developed to address the boost converter's unstable zero point, proving more effective than feedback control in limiting voltage changes and enhancing system stability when the output filter capacitance was reduced, [8]. Additionally, [9], integrated load current feedforward into the control link using direct power control, leading to a significant improvement in the dynamic response of DC converters and the maintenance of a constant output voltage under sudden load changes, as indicated by experimental and simulation results. Furthermore, [10], introduced the establishment of a ripple compensation connection via load current feedforward to enhance the quality of the systematic output power and accelerate the inner loop dynamic reaction time of the existing inner loop control. While the current feedforward control approach mentioned above somewhat enhances the system's dynamic reaction capability, it still faces the challenge of voltage and current loop delay, resulting in a slower response of the output current to the load disturbance.

The power feedforward control method is employed to mitigate bus voltage fluctuations by introducing disturbance power into the control pathway, [11]. A compensation control strategy utilizing power feedforward is implemented alongside classical dual closed-loop control to address bus voltage fluctuations arising from the mismatch between output power and renewable energy load consumption in the microgrid, [12]. This method channels power disturbances into the controller through the feedforward channel, effectively constraining bus voltage fluctuations and enhancing overall system stability. Additionally, [13], proposed a practical direct power control strategy related to direct power feedforward control, improving the bidirectional DC/DC converter's resilience to load disturbances. This eliminates the need to consider the energy storage inductance of the converter and changing ratio parameters of the transformer, thereby enhancing overall system compatibility. Moreover, power feedforward aids in the system's quicker response to power disturbances, thereby enhancing its capability to regulate bus voltage fluctuations to some extent. However, it is essential to note that power feedforward, like current feedforward, must pass through the current inner loop, resulting in some delay in the output current compared to the load disturbance.

Furthermore, it's crucial to acknowledge that feedforward control necessitates real-time monitoring of system parameters, which increases system costs and reduces reliability. This is not conducive to the expansion of the microgrid or the widespread adoption of plug-and-play capabilities, [14]. To address the issues with feedforward control, the use of a state observer eliminates the need for an exact mathematical model that includes the disturbance signal when evaluating the amount of disturbance. This approach simplifies model construction, avoids complex mathematical calculations, and meets the real-time property requirements of the system. However, the use of an observer to monitor the system's state variables introduces noise, despite the relatively simple models

2 Microgrid Description

The microgrid under examination in this study operates at a voltage level of 48 volts, as illustrated in Figure 1. During island mode, the maintenance of power balance is achieved by regulating the distributed energy sources and compensating devices. The microgrid consists of three DC buses, each associated with its respective subsystem and controlled by a regional controller (RC). Loads are connected to each bus and distributed across the system.

2.1 About Photovoltaic System (PV) System

The PV system is connected to the bus and is subjected to variations in temperature and irradiance. It is also equipped with battery storage. A boost converter is employed for maximum power point tracking (MPPT) to optimize the array's power output. This converter utilizes the incremental conductance (InC) approach and an additional integral regulator for robustness. Advanced MPPT techniques may be employed when necessary. According to the InC method, the derivative of the module power is assumed to be zero at the MPPT, positive to the left of the MPP, and negative to the right of the MPP, [15]. The InC technique concludes its search for the applied PV voltage when the system's InC and system conductance are equal, corresponding to the lowest rate of change in PV power (Ppv). This can be mathematically represented.

$$\frac{dP_{PV}}{dV_{PV}} \approx 0 \tag{1}$$

Substituting for $P_{pv} = V_{pv} I_{pv}$ in (1), we get

$$\frac{d\left((V_{PV})(I_{PV})\right)}{dV_{PV}} \approx 0 \tag{2}$$

$$I_{PV}\frac{dV_{PV}}{dV_{PV}}+V_{PV}\frac{dI_{PV}}{dV_{PV}}\approx 0 \quad (3)$$

$$I_{PV}+V_{PV}\frac{dI_{PV}}{dV_{PV}}\approx 0 \quad (4)$$

$$\frac{dI_{PV}}{dV_{PV}}=-\frac{I_{PV}}{V_{PV}} \quad (5)$$

The DC-DC converter, based on the InC algorithm, is responsible for adjusting the operating point of the PV array to satisfy equation (5). The battery regulates the voltage of the bus, operating its converter in a constant voltage mode. Consequently, the converter can operate in constant current mode (CCM), delivering the microgrid with the maximum achievable power output. Any surplus energy generated is stored in the battery, enabling the PV system to operate continuously in MPPT mode.

Figure 2 illustrates a detailed diagram of the subsystem. The unidirectional converter of the PV panel operates in MPPT mode, while the bidirectional converter of the battery regulates the bus voltage using a proportional-integral (PI) controller. Excess power in the microgrid is directed towards charging the battery storage, and the charging current is controlled to sustain a constant bus voltage

2.2 GaN Bidirectional DC/DC Converter

DC-DC power converters play a crucial role in DC microgrid systems, as they convert electricity from various voltage levels to the required output voltage level. However, traditional DC converters only facilitate unidirectional power transfer, limiting bidirectional power flow. To overcome this limitation, the proposed solution involves the use of advanced power devices, specifically Gallium Nitride High Electron Mobility Transistors (GaN HEMT), known for their enhanced static and dynamic properties, thereby improving the efficiency of power converters.

GaN devices surpass their Silicon (Si) counterparts in key aspects such as lower output capacitance, absence of reverse recovery effects, and low on-state resistance, contributing to an overall enhanced performance, [16], as depicted in Figure 3. This implementation facilitates the charging and discharging of storage devices like batteries and supercapacitors. Not only does this streamline the process, but it also allows for more effective utilization of stored energy, enhancing the overall adaptability and robustness of the system

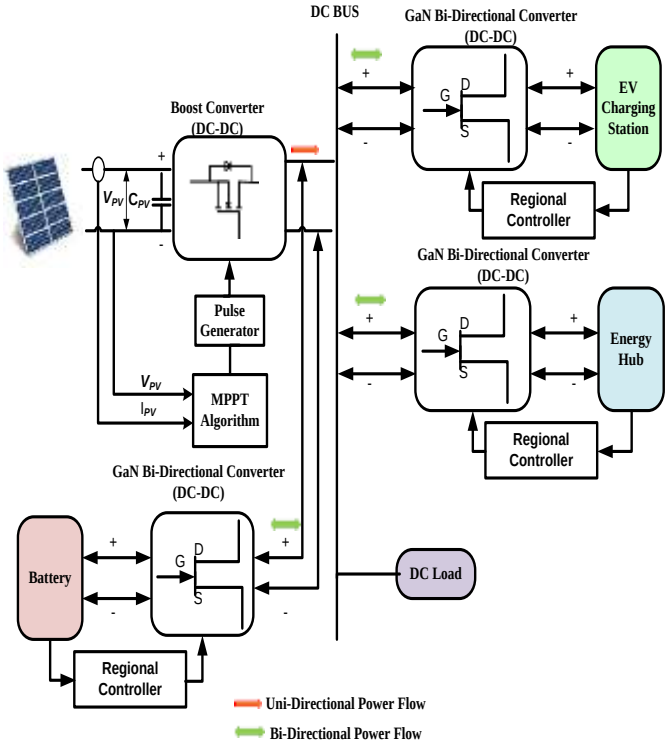

Fig. 1: Solar PV-based DC microgrid System

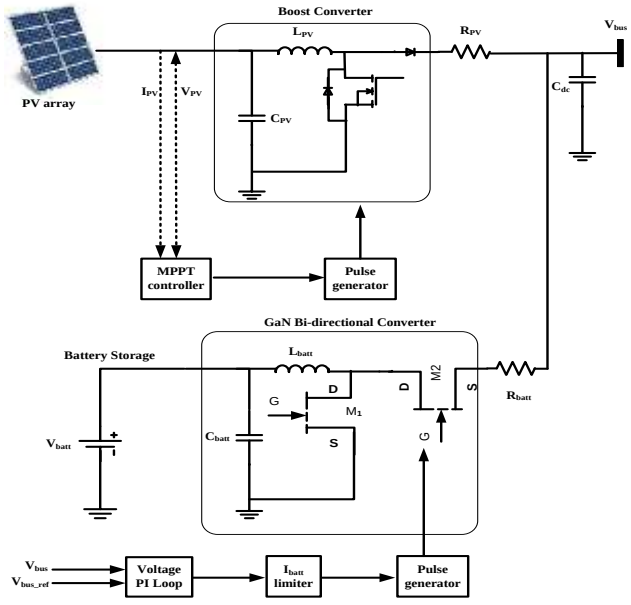

Fig. 2: Implemented PV-battery system.

The dynamic model of the converter incorporates parasitic resistances identified as RL and RC, to characterize the inductor and capacitor characteristics, respectively.

The state-space model of the converter can be represented as equations (6) and (7), where the system matrices are denoted as A, B, C, and D.

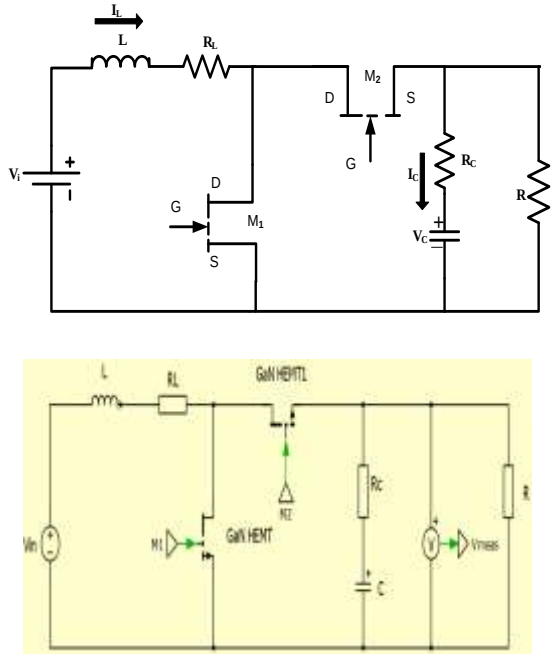

Fig. 3: Implemented GaN bidirectional DC-DC converter with PLECS Software

$$x^{|} = Ax + Bu \tag{6}$$

$$y = Cx + Du \tag{7}$$

The state-space model (SSM) of the converter can be obtained by averaging two discrete SSMs. The first SSM is associated with the scenario when M1 is ON and M2 is OFF for a duty cycle of d1, as depicted in equation (8). The second SSM corresponds to the situation when M1 is OFF and M2 is ON for a duty cycle of d2, equal to 1 minus d1, as illustrated in equation (9). The chosen state variables are iL and Vc, denoted by x1 and x2, respectively.

$$x'_{d1} = \begin{pmatrix} \frac{-R_L}{L} & 0 \\ 0 & \frac{-1}{C(R+R_C)} \end{pmatrix} x + \begin{pmatrix} \frac{1}{L} \\ 0 \end{pmatrix} u \tag{8}$$

$$x'_{d2} = \begin{pmatrix} \frac{1}{L}\left(R_L + \frac{RR_C}{R+R_C}\right) & \frac{-1}{L}\left(1+\frac{R_C}{R+R_C}\right) \\ \frac{R}{C(R+R_C)} & \frac{-1}{C(R+R_C)} \end{pmatrix} x + \begin{pmatrix} \frac{1}{L} \\ 0 \end{pmatrix} u \tag{9}$$

Equations (10) and (11) can be employed to derive the averaged state-space model (SSM), yielding equation (12).

$$A = d_1 A_1 + d_2 A_2 \tag{10}$$

$$B = d_1 B_1 + d_2 B_2 \tag{11}$$

$$\begin{pmatrix} \frac{1}{L}\left(R_L(1-2d) + \frac{R.R_C}{R+R_C}.d'\right) & \frac{-1}{L}\left(1+\frac{R_C}{R+R_C}\right).d' \\ \frac{R(1-d)}{C(R+R_C)} & \frac{-1}{C(R+R_C)} \end{pmatrix} x + \begin{pmatrix} \frac{1}{L} \\ 0 \end{pmatrix} u \tag{12}$$

Similarly, the matrices C and D can be derived, leading to equation (13) as shown below

$$y = \begin{pmatrix} 1 & 0 \\ 0 & 1 \end{pmatrix} x + \begin{pmatrix} \frac{1}{L} \\ 0 \end{pmatrix} u \tag{13}$$

The obtained averaged state-space model (SSM) illustrates the performance of the converter throughout a complete cycle with a period of Ts.

2.3 Energy Hub System

Microgrids necessitate power compensation systems due to the inconsistent nature of renewable energy sources and changing demands. These systems serve two primary purposes: firstly, to function as a power source when microgrid generation is inadequate to meet load demand, and secondly, to act as a power sink when generation exceeds demand. While traditional battery storage serves as one method of compensation, its slow dynamic response is insufficient for rapid changes in load or renewable power. In contrast, supercapacitors (SCcap) offer advantages such as rapid response time and high instantaneous output power. Previous studies have emphasized the benefits of incorporating supercapacitors in various components of microgrids, [17].

The proposed design aims to integrate Energy Hubs into the microgrid system for two primary purposes. Firstly, to ensure smooth power delivery during peak demand periods, the supercapacitor is utilized to absorb strong transients. Secondly, to maintain bus voltage, the battery system is employed. Typically, power regulation and balancing in microgrids are managed through generation unit outputs, such as PV units. However, during peak demand periods, generation units must operate at their maximum capacity, which can be challenging. Introducing an Energy Hub can alleviate the pressure on the generation units and transfer control to other parts of the system, making it more efficient and reliable.

As depicted in Figure 4, the Energy Hub consists of a SCap coupled to the same DC bus using bidirectional converters. The SCap control employs a cascaded PI system with an outer voltage loop and an inner current loop, while the battery control regulates the bus voltage. The supercapacitor

control ensures that the isc value is zero during a steady state.

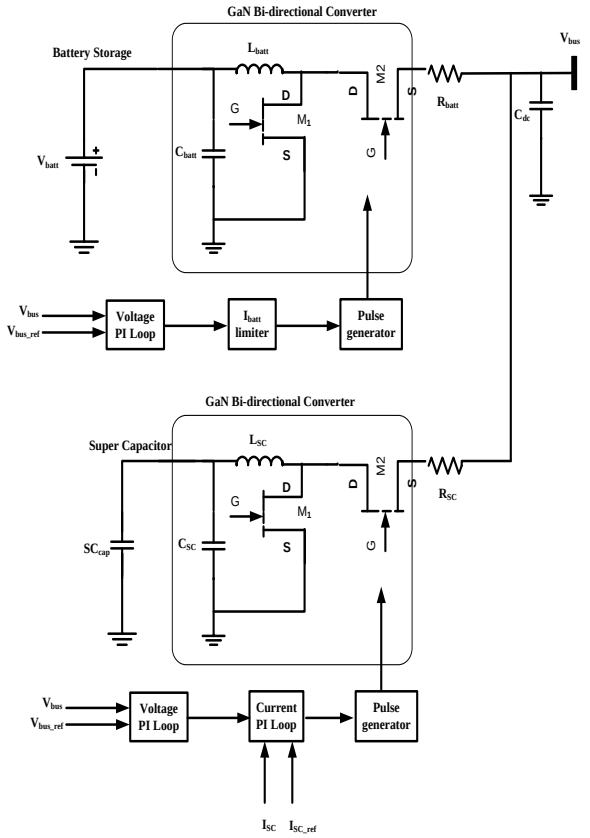

Fig. 4: Implemented energy hub system

2.4 About Charging Station of Electric Vehicle

The integration of vehicle-to-grid (V2G) technology into microgrids has opened up new possibilities for transferring the compensation load to electric vehicles connected to charging stations. The benefits and challenges of adopting this technology have been thoroughly analyzed in previous studies, [18]

Within the microgrid under examination, the charging station is linked to the bus, and its main function is to recharge the electric vehicles (EVs) that connect to it. However, during periods of peak demand, the EVs can also operate as a power source to assist in regulating the microgrid. The DC voltage at the bus is adjusted by modifying the value of Vev, which occurs when multiple EVs connect or disconnect from the charging station node, as illustrated in Figure 5.

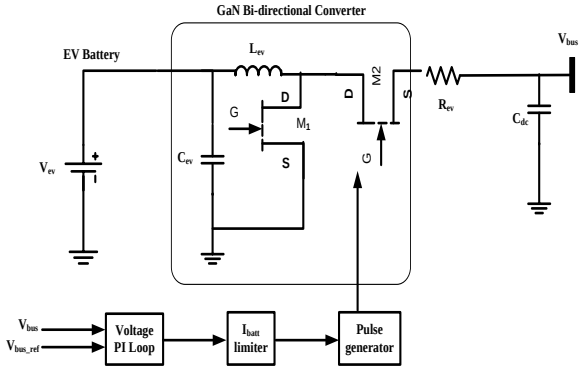

Fig. 5: Implemented EV charging station system

3 Proposed Control Technique

The objective of this article is to introduce a method for energy optimization in a DC decentralized power network using a distributed control technique. This approach does not depend on a communication network. Instead, power flow from individual sources is regulated through interconnected DC/DC converters.

3.1 PI Controller

The PI controller generates the required duty cycle based on the output error, similar to the PID controller. However, the PI controller is significantly less susceptible to disturbances and produces an oscillation-free duty cycle. Moreover, the PI controller outperforms the PID controller in terms of offset and steady-state error, [19]. Consequently, this paper employs a PI controller instead of a PID controller, considering these factors. The mathematical analysis of the PI controller is shown in the equation below.

$$U(t) = K_i \int_0^t e(t)\,dt + K_p e(t) \tag{14}$$

The error signal e(t) is the difference between the bus value and the reference signal Voltage (Vbus) and reference voltage (Vbus_ref).

$$e(t) = V_{bus} - V_{bus\_ref} \tag{15}$$

The dual-loop control method involves the use of two PI controllers - one for the voltage loop and the other for the current loop. The first controller receives direct feedback from the converter's output and its output is then passed on and transferred to the second controller, which creates the necessary duty cycle. Here Table 1 shows the gain values of the PI controller related to mode of operation pertaining to the type of energy source utilized to drive the electric vehicle.

Table 1. PI control Parameters

Mode	K_{pv}	K_{iv}	K_{pi}	K_{ii}
Battery	0.2	2.45	0.45	2.8
Supercapacitor	0.1	4	0.27	3.2
PV-Battery	0.1	4	10	4

When converter parameters, such as input voltage and output current, are influenced by nonlinear or continually changing conditions, and output filter performance is involved, tuning the PI controller becomes a cumbersome and time-consuming task. Moreover, conventional PI tuning lacks a right-half-plane zero, leading to a restricted understanding of the converter's behavior, [19].

3.2 Fuzzy Logic Controller

The effectiveness of Fuzzy Logic Control (FLC) heavily relies on the rules defined by linguistic variables, and unlike other approaches, it doesn't require intricate arithmetic operations. It conducts simple calculations to regulate the model, making it one of the most effective and accessible methods for plant regulation. FLC, grounded in fuzzy set theory, assigns membership levels to elements, reflecting their association with specific sets characterized by less well-defined boundaries compared to classical sets. Despite its reliance on basic mathematics, FLC excels in control systems, especially when precision requirements are minimal.

The FLC excels in providing an optimal switching sequence for the charging and discharging operations of batteries. It receives error indications from the DC Bus voltage compared to the reference voltage signal. Utilizing this information, the fuzzy controller determines the duty cycle for the PWM block, thereby signaling the buck/boost converter.

This study employs FLC with a Mamdani base, taking two inputs: the output voltage error (e(t)) and the change in error (de(t)) from the previous error. The definitions of e(t) and de(t) are provided in the subsequent equations.

$$e(t) = V_{sense}(t) - V_{ref} \tag{16}$$

$$de(t) = e(t) - e(t-1) \tag{17}$$

In this context, Vref represents the desired output voltage, and Vsense(t) is the tth sampled output voltage of the system. Both input variables are multiplied by scaled factors k1 and k2 before being fed into the Fuzzy Logic Controller (FLC). Subsequently, the scaled input undergoes membership function (MF) assignment based on fuzzy logic rules. Triangular MF is selected for its simplicity and ease of application, despite various MF shapes being available. While a larger number of fuzzy sets is beneficial for smooth system adjustment, it also adds complexity to MF forms. Thus, there exists a trade-off between the complexity of the MF and the quantity of fuzzy sets employed. The FLC is allocated seven fuzzy subsets, named NL, NM, NS, ZE, PS, PM, and PL, where L, M, and S denote big, medium, and small, respectively, and N, P, and Z represent negative, positive, and zero, respectively. The FLC outputs the required duty cycle (D), which is then transmitted to the plant. Fuzzy control rule sets are defined based on a 7x7 converter matrix. Figure 6 depicts the block diagram representation of the fuzzy logic controller.

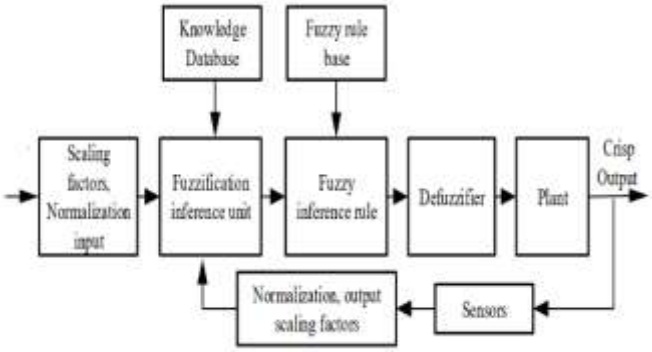

Fig. 6: Block diagram of FLC

3.3 Gallium Nitride HEMT Transistor

In the realm of a Zero Voltage Switching (ZVS) configuration, medium, and high-voltage Silicon (Si) Metal-Oxide-Semiconductor Field-Effect Transistors (MOSFETs) showcase heightened switching losses and intermittent operational glitches, as extensively documented in the literature, [20], [21]. The extended reverse recovery duration exhibited by the intrinsic body diode under conditions of low reverse voltage stands out as the primary instigator of these adverse MOSFET failures, [22]. It is pivotal to underscore that once the body diode enters the reverse recovery phase, it can trigger the failure mode through either the peak reverse recovery current (IRRM) or the rate of voltage change during the turn-off process (dv/dt). These complications stem from the intrinsic structural properties of super-junction MOSFETs, which are differentiated by a greatly increased PN junction area. Despite iterative improvements, the persistence of this poor reverse recovery phenomena remains a long-term and severe obstacle.

Furthermore, it is critical to emphasize that when there is little or no load, another failure mechanism

occurs inside Zero Voltage switching (ZVS) super-junction Metal-Oxide-Semiconductor Field-Effect Transistors (MOSFETs). The parasitic output capacitor remains partly charged in this circumstance, surviving exceeding voltage levels of zero. Surprisingly, despite efforts to mitigate the intrinsic diode recovery effects, this difficulty persists. This phenomenon, known as the "Cdv/dt shoot-through issue," happens only within the leg allocated for short-circuiting.

To complicate matters further, the energy that has been stored within the resulting capacitor evaporates as it passes into the device after activation, adding another layer of complication to the problem. Notably, the non-linear properties of the output capacitance (Coss) create a strong barrier to attaining Zero Voltage Switching (ZVS). This large barrier stems from the fact that the power MOSFET's output capacitor increases exponentially as the drain-source voltage approaches zero. As a result, the issue of quickly draining the output capacitance is exacerbated, eventually leading to longer discharge intervals.

In general, Silicon (Si) MOSFETs have several flaws including a long reverse recovery time, a significant reverse recovery charge, and a large output capacitance. These combined features signify a sluggish switching speed and elevated switching losses. Therefore, in the selection of a power switch for integration into a bidirectional converter, it becomes paramount that the chosen power switch exhibits the following fundamental characteristics [22]:

a) Fast reverse recovery of body diode especially at lower reverse voltage;
b) Less reverse recovery charge of body diode;
c) Less output capacitance *Coss*;
d) Less *Qgd/Qgs* ratio;
e) High threshold voltage.

Figures of Merit (FOMs) serve as valuable tools for evaluating and comparing device performance, particularly during early design phases, [23], [24], [25], [26]. Earlier studies introduced FOMs tailored for hard-switching and soft-switching applications, [23]. These metrics consistently illustrate that Gallium Nitride High Electron Mobility Transistors (GaN HEMTs) outperform Silicon (Si) Metal-Oxide-Semiconductor Field-Effect Transistors (MOSFETs) in high-frequency and high-voltage scenarios, encompassing both hard and soft-switching circuits, about conduction and switching losses.

Furthermore, a novel Figure of Merit (FOM) crafted to assess reverse-recovery characteristics during synchronous rectification was introduced, [24]. A thorough comparison in [25], between 650V GaN HEMTs and Si MOSFETs consistently favored GaN HEMTs across both FOMs. This heightened performance can be ascribed to the inherent properties of GaN HEMTs, notably the absence of minority carriers in conduction, leading to the elimination of reverse recovery charge. Nevertheless, similar to Si MOSFETs, it remains imperative to minimize body diode conduction. In these applications, GaN devices demonstrate exceptional performance.

4 Results and Discussion

The suggested control approach was evaluated for its ability to regulate bus voltage and optimize load balancing with both effectiveness and precision and tested for resilience under various scenarios. Detailed descriptions of the outcomes for each test can be found in the subsequent sections.

4.1 Dynamic Load Changes

The efficacy of the suggested power management system was assessed for sudden changes in load characterized by a rapid increase and subsequent decline with PI controller with GaN converter. During these tests, regional controllers employed their specific control algorithms to counteract bus voltage fluctuations. As power generation decreased, the Energy Hub introduced power into the microgrid, with the supercapacitor handling abrupt power transients until the batteries could achieve the new steady-state value. The outcomes are depicted in Figure. 7 indicates that the Fuzzy control approach handles sudden changes in load proficiently, ensuring effective bus voltage and power regulation

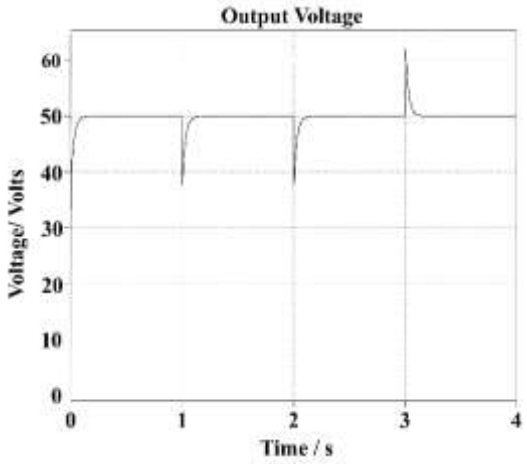

(a)

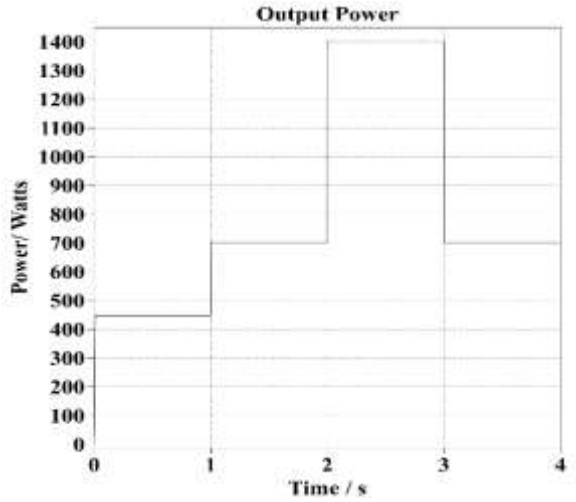

(b)

Fig. 7: PLECS Simulation results with Step-load change in (a) Voltage (b) Power

4.2 Communication Delay

The control method proposed in this study was tested for its ability to respond to controller communication delays in a distributed microgrid mode. A 200 ms communication latency was imposed between each regional controller in the system, and the strategy was simulated.

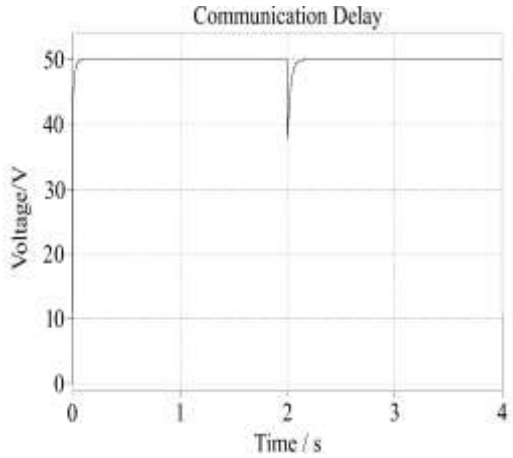

Fig. 8: PLECS Simulation with a communication delay of 200 ms

The results are presented in Figure 8, where the suggested Fuzzy control method with GaN converter demonstrates faster voltage stabilization, with a voltage stabilization time of 0.15 s. This suggests that the projected control can stabilize bus voltage even if there is a communication delay between the regional controllers due to the distributed mode.

5 Conclusions

In this paper, the GaN-based bidirectional DC-DC converter is proposed for a microgrid. The paper applies the fuzzy controller technique in the microgrid, which depends upon a bidirectional DC-DC converter-based Hybrid Energy Storage System (HESS) to enhance the stability of the DC voltage. Specifically, solar energy is considered as the input source to provide continuous power to the microgrid. Both the Supercapacitor (SC) and Battery units within the HESS are charged by solar energy.

The GaN-based converter system's performance was assessed using PLECS Software. It was determined that the proposed approach can effectively control the bus voltage at the desired level and rapidly regulate the output power in response to changes in the reference or load. This study suggests that the envisioned technique can be efficiently applied within a DC microgrid to ensure voltage stability for Electric Vehicle charging applications.

References:

[1] Zongfei Wang, Patrick Jochem, Wolf Fichtner, "A scenario-based stochastic optimization model for charging scheduling of electric vehicles under uncertainties of vehicle availability and charging demand," *Journal of Cleaner Production*, Vol. 254, 2020, Article 119886, ISSN: 0959-6526, https://doi.org/10.1016/j.jclepro.2019.119886.

[2] Yeqin Wang, Beibei Ren, Sanka Liyanage, "Unified control scheme for a dual-stage grid-connected PV system with mode change", *Solar Energy*, Vol. 239, 2022, pp.88-101, ISSN: 0038-092X, https://doi.org/10.1016/j.solener.2022.04.053.

[3] E. Espina, J. Llanos, C. Burgos-Mellado, R. Cárdenas-Dobson, M. Martínez-Gómez and D. Sáez, "Distributed Control Strategies for Microgrids: An Overview," in *IEEE Access*, vol. 8, pp.193412-193448, 2020, https://doi.org/10.1109/ACCESS.2020.3032378.

[4] D. Xu, J. Liu, X. G. Yan, and W. Yan, "A novel adaptive neural network constrained control for a multi-area interconnected power system with hybrid energy storage," *IEEE Transactions on Industrial Electronics*, vol. 65, no. 8, pp.6625–6634, Aug. 2018, https://doi.org/10.1109/TIE.2017.2767544.

[5] Punna, S.; Mailugundla, R.; Salkuti, S.R. Design, Analysis and Implementation of

Bidirectional DC–DC Converters for HESS in DC Microgrid Applications. *Smart Cities* 2022, Vol. 5, Issue 2, pp.433-454, https://doi.org/10.3390/smartcities5020024.

[6] R. Katuril and S. Gorantla, "Comparative analysis of controllers for a smooth switching between battery and ultracapacitor applied to E-vehicle," *European Journal of Electrical Engineering*, vol. 20, no. 1, pp.47–75, Feb. 2018, doi: 10.3166/ejee.20.47-75.

[7] Iqbal, M.M., Kumar, S., Lal, C. Chandra Kumar "Energy management system for a small-scale microgrid". *Journal of Electrical Systems and Inf. Technol.*, 9, 5 (2022), https://doi.org/10.1186/s43067-022-00046-1.

[8] Shota Miyoshi, Wataru Ohnishi, Takafumi Koseki, Motoki Sato,"Modified preactuation tracking control for LPV systems with application to boost converters", *IFAC-Papers OnLine*, Vol. 53, Issue 2, 2020, pp.7319-7324, ISSN: 2405-8963, https://doi.org/10.1016/j.ifacol.2020.12.985.

[9] Duy-Dinh Nguyen, Dinh-Hoa Nguyen, Minh C. Ta, Goro Fujita, "Sensorless Feedforward Current Control of Dual-Active-Bridge DC/DC Converter for Micro-Grid Applications", *IFAC-Papers OnLine*, Vol. 51, Issue 28, 2018, pp.333-338, ISSN: 2405-8963, https://doi.org/10.1016/j.ifacol.2018.11.724.

[10] Hoyos Velasco, C.I.; Hoyos Velasco, F.E.; Candelo-Becerra, J.E. Nonlinear Dynamics and Performance Analysis of a Buck Converter with Hysteresis Control. *Computation* 2021, *9*, 112, https://doi.org/10.3390/computation9100112.

[11] Saha, Akshay Kumar, Pon Ragothama Priya, P. Baskar, S., Tamil Selvi, S., Babulal, C. K., 2023/05/27, "Optimal Allocation of Hybrid Renewable Distributed Generation with Battery Energy Storage System Using MOEA/D-DRA Algorithm", *International Transactions on Electrical Energy Systems*, 7316834, 2023, 2050-7038, https://doi.org/10.1155/2023/7316834.

[12] Magaldi, G.L.; Serra, F.M.; de Angelo, C.H.; Montoya, O.D.; Giral-Ramírez, D.A. Voltage Regulation of an Isolated DC Microgrid with a Constant Power Load: A Passivity-based Control Design. *Electronics* 2021, *10*, 2085, https://doi.org/10.3390/electronics10172085.

[13] W. Song, N. Hou, and M. Wu, "Virtual direct power control scheme of dual active bridge DC-DC converters for fast dynamic response," *IEEE Transactions on Power Electronics*, vol. 33, no. 2, pp.1750–1759, Feb. 2018, https://doi.org/10.1109/TPEL.2017.2682982.

[14] Trinh H-A, Nguyen DG, Phan V-D, Duong T-Q, Truong H-V-A, Choi S-J, Ahn KK. Robust Adaptive Control Strategy for a Bidirectional DC-DC Converter Based on Extremum Seeking and Sliding Mode Control. *Sensors*. 2023; 23 (1), 457, https://doi.org/10.3390/s23010457.

[15] Ogang Qu, Zidong Wang, Bo Shen, Hongli Dong, "Distributed state estimation for renewable energy microgrids with sensor saturations", *Automatica*, Vol. 131, 2021, 109730, ISSN: 0005-1098, https://doi.org/10.1016/j.automatica.2021.109730.

[16] He, J.; Chen, Y.; Lin, J.; Chen, J.; Cheng, L.; Wang, Y. Review of Modeling, Modulation, and Control Strategies for the Dual-Active-Bridge DC/DC Converter. *Energies* 2023, *16*, 6646, https://doi.org/10.3390/en16186646.

[17] Tareq Salameh, Mohammad Ali Abdelkareem, A.G. Olabi, Enas Taha Sayed, Monadhil Al-Chaderchi, Hegazy Rezk, "Integrated standalone hybrid solar PV, fuel cell and diesel generator power system for battery or supercapacitor storage systems in Khorfakkan", United Arab Emirates, *International Journal of Hydrogen Energy*, Vol. 46, Issue 8, 2021, pp.6014-6027, ISSN: 0360-3199, https://doi.org/10.1016/j.ijhydene.2020.08.153

[18] Bijan Bibak, Hatice Tekiner-Moğulkoç, A comprehensive analysis of Vehicle to Grid (V2G) systems and scholarly literature on the application of such systems, *Renewable Energy Focus*, Vol. 36, 2021, pp.1-20, ISSN: 1755-0084, https://doi.org/10.1016/j.ref.2020.10.001.

[19] Toub M, Bijaieh MM, Weaver WW, Robinett RD III, Maaroufi M, Aniba G. "Droop Control in DQ Coordinates for Fixed Frequency Inverter-Based AC Microgrids". *Electronics*. 2019; 8(10):1168, https://doi.org/10.3390/electronics8101168.

[20] S. Chi, P. Liu, X. Li, M. Xu and S. Li, "A Novel Dual Phase Shift Modulation for Dual-Active- Bridge Converter," *2019 IEEE Energy Conversion Congress and Exposition (ECCE)*, Baltimore, MD, USA, 2019, pp. 1556-1561, https://doi.org/10.1109/ECCE.2019.8912591.

[21] Lyu, D., Straathof, C., Soeiro, T. B., Qin, Z., & Bauer, P. (2023). ZVS-Optimized Constant and Variable Switching Frequency

Modulation Schemes for Dual Active Bridge Converters. *IEEE Open Journal of Power Electronics*, 4, pp.801-816, https://doi.org/10.1109/OJPEL.2023.3319970.

[22] Kumar, Vikram and Vipan Kakkar. "A Review on Control Strategies of Dual Active Bridge-Isolated Bidirectional DC-DC Converter for High Frequency Power Conversion Systems." *JETIR*, 2021, Vol. 8, Issue 2, ISSN: 2349-5162.

[23] Ahmed, Osama, Yousuf Khan, Muhammad A. Butt, Nikolay L. Kazanskiy, and Svetlana N. Khonina. 2022. "Performance Comparison of Silicon- and Gallium-Nitride-Based MOSFETs for a Power-Efficient, DC-to-DC Flyback Converter" *Electronics,* 11, no. 8: 1222, https://doi.org/10.3390/electronics11081222.

[24] B. J. Baliga, "Integral Diode," in *Advanced Power MOSFET Concepts*. New York, NY: Springer, 2010, ch. 8, sec. 4, pp. 472–476, DOI: 10.1007/978-1-4419-5917-1

[25] Shishir S. Trivedi, Amit V. Sant, Comparative analysis of dual active bridge dc–dc converter employing Si, SiC and GaN MOSFETs for G2V and V2G operation, *Energy Reports*, Vol. 8, Supplement, 13, 2022, pp.1011-1019, ISSN: 2352-4847, https://doi.org/10.1016/j.egyr.2022.08.100.

[26] Ma, Chao-Tsung, and Zhen-Huang Gu. 2019. "Review of GaN HEMT Applications in Power Converters over 500 W", *Electronics*, 8, no. 12: 1401. https://doi.org/10.3390/electronics8121401.

Contribution of Individual Authors to the Creation of a Scientific Article (Ghostwriting Policy)

The authors equally contributed in the present research, at all stages from the formulation of the problem to the final findings and solution.

Sources of Funding for Research Presented in a Scientific Article or Scientific Article Itself

No funding was received for conducting this study.

Conflict of Interest

The authors have no conflicts of interest to declare**.**